Analysis and Control Parameter Estimation of a Tubular Linear Motor with Halbach and Radial Magnet Array

Seok-Myeong Jang*, Jang-Young Choi†, Han-Wook Cho* and Sung-Ho Lee**

Abstract - In the machine tool industry, direct drive linear motor technology is an interesting means to achieve high acceleration, and to increase reliability. This paper analyzes and compares the characteristics of a tubular linear motor with Halbach and radial magnet array, respectively. First, the governing equations are established analytically in terms of the magnetic vector potential and two dimensional cylindrical coordinate systems. Then, we derive magnetic field solutions due to the PMs and the currents. Motor thrust, flux linkage and back emf are also derived. The results are shown to be in good conformity with those obtained from the commonly used finite element method. Finally, control parameters are obtained from analytical solutions.

Keywords: Tubular linear motor, Halbach and radial magnet array, Analytical solutions.

1. Introduction

Our work is motivated by the desire to develop a direct drive linear motor for machine tool applications. The applications for such a motor range from material handling devices to semi-conductor wafer stepping functions, diamond turning machines and other precision applications [1]. Tubular structures are very advantageous compared with flat linear motors, owing to the non-existence of end-turn effects. In addition to this benefit, the tubular motor provides many other advantages: 1) higher maximum speeds and acceleration limits, 2) higher position accuracy without anti-backlash devices, 3) no direct physical constraint in the axial direction of propulsion, 4) no power loss in rotary-linear power conversion and, 5) no friction except in the ball bearings that support the platen weight [1].

In this paper, two PM tubular motor structures are analyzed. One is the tubular motor with the Halbach magnet array and the other is the tubular motor with the radial magnet array. Two types of PM tubular motors are analyzed, with reference to the following parameters as variables: magnetic fields, flux linkage, motor thrust and back emf. These variables are derived by the use of analytical method in terms of the two-dimensional cylindrical coordinate system. The results are validated extensively by comparison with the finite element method. Finally, control parameters such as thrust constant, back emf constant and inductance are obtained from analytical solutions.

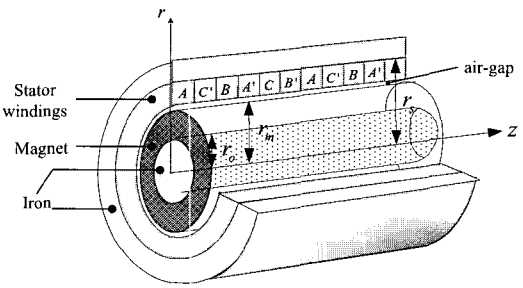

Fig. 1 Schematic of tubular linear motor.

2. Tubular Linear Motor with Halbach and Radial Magnet Array

2.1 Structures

Fig. 1 presents the schematic of a tubular linear motor. It consists of the PMs as a mover, a coil-wrapped hollow bobbin, and an iron core as a pathway for the magnetic flux. When stator windings are excited, the mover moves in the direction of z. The 3-phase stator windings shown in Fig. 1 can be replaced by single phase windings.

2.2 Analytical model and assumptions

Fig. 2 shows the analytical model for the prediction of flux density produced by PMs of the tubular linear motor

† Corresponding Author: Department of Electrical Engineering, Chungnam National University, Daejeon, 305-764, Korea (aramis76@cnu.ac.kr).
* Department of Electrical Engineering, Chungnam National University, Daejeon, 305-764, Korea(smjang@cnu.ac.kr, hwcho@cnu.ac.kr).
**LG Digital Appliance Lab., 327-23, Gasandong, Gumchun-gu, Seoul, Korea(iemechas@lge.com).
Received May 6, 2004 ; Accepted August 26, 2004

with Halbach and radial array. The radii shown relate to the inner magnet radius, r_o, the outer magnet radius, r_m and the outer stator windings radius, r_s. Assuming that the relative recoil permeability of the winding regions and the iron is unity and infinite, respectively, the magnetic field analysis due to PMs is confined to two regions represented as the air region

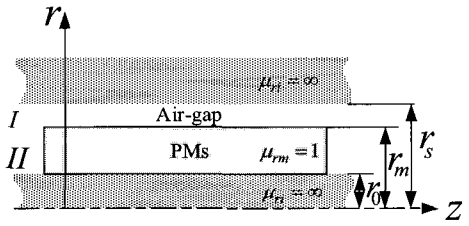

Fig. 2 Analytical model for the prediction of flux density produced by PMs of tubular linear motor with Halbach and radial array.

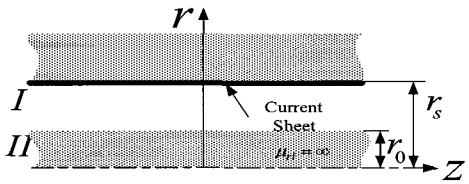

Fig. 3 Analytical model for the prediction of flux density due to single and three phase current density distribution.

and the magnet regions. Therefore,

$$\vec{B} = \begin{cases} \mu_0 \vec{H} & \text{in the air/stator windings} \\ \mu_0 \mu_{rm} \vec{H} + \mu_0 \vec{M} & \text{in the magnets} \end{cases} \quad (1)$$

where μ_0 is the permeability of the air; μ_{rm} is the relative recoil permeability of the magnets and is supposed unity; $\vec{M}$ is the remanent magnetization. Fig. 3 presents the analytical model for the prediction of flux density due to single and three phase windings. In order to predict the flux density due to stator windings, this paper assumes that the stator current flows through an infinitesimally thin sheet on the interior surface of the stator, at $r=r_s$ and both iron permeability and motor length are infinite.

3. Magnetic Fields Due to the PMs

3.1 Impulse magnetization technique

By assuming that radial magnet array has only radial components of magnetization and is rectangular shaped along the axial coordinate, it is conveniently expressed by means of the Fourier series expansion for radial magnetization given by

$$\overrightarrow{M_r} = \sum_{n=1,odd}^{\infty} M_n \sin(k_n z)\vec{i}_r \quad (2)$$

with k_n=nπ/τ and

$$M_n = \frac{4B_{rem}}{n\pi\mu_0}\sin(n\pi/2)\sin(k_n\tau_m) \quad (3)$$

where n is the nth-order harmonics; τ and τ_m represent pole pitch of motor and magnet, respectively; and B_{rem} is the PM residual flux density. However, radial magnetization is a function only of the axial coordinate, as shown in (1). It is slightly altered, allowing it to function by both radial and axial coordinates through the introduction of function G(r) presented in [2]. As a consequence, the Fourier series expansion for radial magnetization is modified by

$$\overrightarrow{M_r} = \left(\frac{c_1}{r} + c_2 r\right) \cdot \sum_{n=1,odd}^{\infty} M_n \sin(k_n z)\vec{i}_r \quad (4)$$

where the coefficients c_1 and c_2 are given in [2]. In a similar manner, the Fourier series expansion for Halbach magnetization is given by

$$\overrightarrow{M_H} = \sum_{n=1,odd}^{\infty}\left[\left(\frac{c_1}{r} + c_2 r\right)M_{rn}\vec{i}_r + M_{zn}\vec{i}_z\right]\sin(k_n z) \quad (5)$$

where the radial and axial components of Halbach magnetization are given by

$$M_{rn} = \frac{4B_{rem}}{n\pi\mu_0}\sin(n\pi/2)\sin(k_n\tau_m) \quad (6)$$

$$M_{zn} = \frac{4B_{rem}}{n\pi\mu_0}\sin(n\pi/2)\cos(k_n\tau_m) \quad (7)$$

3.2 Governing Equations

Since there is no free current in the magnet region, $\nabla \times \vec{H} = 0$. So, $\nabla \times \vec{B} = \mu_0 \nabla \times \vec{M}$. The magnetic vector potential $\vec{A}$ is defined as $\nabla \times \vec{A} = \vec{B}$. By the geometry of the tubular linear motor, the vector potential has only θ-

components. Therefore, Poisson's equation for Halbach and radial magnet array is given by

$$\frac{\partial^2}{\partial r^2}A_{\theta n}+\frac{1}{r}\frac{\partial}{\partial r}A_{\theta n}-\left(k_n^2+\frac{1}{r^2}\right)A_{\theta n}=-\mu_0 k_n\left(\frac{c_1}{r}+c_2 r\right)K \quad (8)$$

where for tubular motor with radial array $K=M_n$, whilst for tubular motor with Halbach array $K=M_{rn}$.

3.3 Characteristic Equations For Flux Density

The resulting axial and radial components of flux density can be determined from general solutions derived in (8) and the definition of magnetic vector potential presented in [3] as follows.

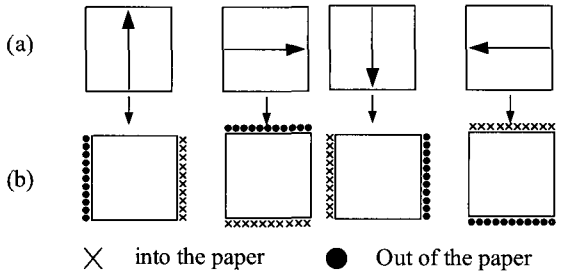

Fig. 4 Electromagnetic dual of Halbach array: (a) Halbach magnet array (b) Equivalent current model.

$$\begin{aligned}
B_{zn}^{I} &= \sum_{n=1,odd}^{\infty} k_n[A_n^I I_0(k_n r)-B_n^I K_0(k_n r)]\cos(k_n z)\\
B_{zn}^{II} &= \sum_{n=1,odd}^{\infty}\left(\begin{array}{l} k_n[A_n^{II} I_0(k_n r)-B_n^{II} K_0(k_n r)\\ \qquad +\dfrac{2c_2\mu_0 K}{k_n^2}]\cos(k_n z)\end{array}\right)\\
B_{rn}^{I} &= \sum_{n=1,odd}^{\infty} k_n[A_n^I I_1(k_n r)+B_n^I K_1(k_n r)]\sin(k_n z)\\
B_{rn}^{II} &= \sum_{n=1,odd}^{\infty}\left(\begin{array}{l} k_n[A_n^{II} I_1(k_n r)+B_n^{II} K_1(k_n r)\\ \qquad +\dfrac{\mu_0 K}{k_n}\left(\dfrac{c_1}{r}+c_2 r\right)]\sin(k_n z)\end{array}\right)
\end{aligned} \quad (9)$$

where I_1 and K_1 are modified Bessel functions of the first and second kind, of order one, and I_0 and K_0 are also modified Bessel functions of the first and second kind, of order zero [4]. Equation (9) can be applied to tubular linear motor with either Halbach or radial magnet array. The coefficients A_n^I, B_n^I, A_n^{II} and B_n^{II} given in the Appendix are only different in each model and are determined by substituting (9) for boundary conditions given by the following section.

3.4 Boundary Conditions

The Halbach magnet array shown in Fig. 4(a) can be expressed as an equivalent current model by applying Ampere's law to it, as presented in Fig. 4(b) [5]. Since the equivalent current for axial components of Halbach magnetization is discontinuous at the upper and lower surface of the permanent magnet, it must be considered. However, for radial magnetization it does not have to be considered owing to the absence of axial magnetized PMs. In addition, the radial flux density is continuous at all interfaces and the axial field intensity is also continuous at all interfaces, except for inner and outer surface of magnets in the case of Halbach magnetization. Due to the assumption that the permeability of the stator core is infinite, the axial field intensity is zero at $r=r_s$ for both Halbach and radial magnetized mover topologies. As a consequence, boundary conditions of the tubular linear motor with Halbach and radial array are given by

Halbach magnetization	radial magnetization
$H_z^{II}(r_o,z)=-M_{zn}$	$H_z^{II}(r_o,z)=0$
$B_r^{II}(r_m,z)=B_r^{I}(r_m,z)$	$B_r^{II}(r_m,z)=B_r^{I}(r_m,z)$
$H_z^{II}(r_m,z)-H_z^{I}(r_m,z)=-M_{zn}$	$H_z^{II}(r_m,z)=H_z^{I}(r_m,z)$
$H_z^{I}(r_s,z)=0$	$H_z^{I}(r_s,z)=0$ (10)

4. Magnetic Fields Due to the Stator Currents

The linear current density $\vec{J}$ is characterized by only the azimuthal component $J_\theta(z)$ function of the axial coordinate, which using the Fourier series expansion can be expressed as

$$J_\theta(z)=\sum_{n=1,odd}^{\infty} J_n\sin(k_n z) \quad (11)$$

where J_n is the function of the current value and the winding distribution. Since this paper assumes that the current is distributed in an infinitesimal thin sheet, both air/stator windings and iron regions remain characterized by curl$H$=0 and then magnetic fields are computed by means of the vector potential. The governing equation is represented by Laplace's equation (8), with K=0.

$$\frac{d^2 A_{\theta n}}{dr^2}+\frac{1}{r}\frac{dA_{\theta n}}{dr}-\left(k_n^2+\frac{1}{r^2}\right)A_{\theta n}=0 \quad (12)$$

The boundary conditions are given by

$$H_z^I(r_s,z)=J_\theta(z)$$

$$\mu_{ri}H_z^I(r_o,z) = H_z^{II}(r_o,z)$$
$$B_r^{II}(r_o,z) = B_r^I(r_o,z) \quad (13)$$

where μ_{ri} is the relative recoil permeability of the iron and is supposed infinity, that is, $\mu_r = \infty$. The resulting expression of the flux density due to windings is given by

$$B_{rnc}^I = \sum_{n=1,odd}^{\infty} \mu_0 k_n[-I_1(k_n r) + \chi_n K_1(k_n r)]\upsilon_n J_n \cos(k_n z)$$
$$B_{znc}^I = \sum_{n=1,odd}^{\infty} \mu_0 k_n[I_0(k_n r) + \chi_n K_0(k_n r)]\upsilon_n J_n \sin(k_n z) \quad (14)$$

where the coefficients χ_n, υ_n are given by

$$\upsilon_n = \frac{1}{k_n[I_0(k_n r_s) + \chi_n K_0(k_n r_s)]} \quad \chi_n = -\frac{I_0(k_n r_o)}{K_0(k_n r_o)}$$

5. Flux Linkages, Back Emf, and Thrust Force

The flux linkage of each phase is given by

$$\lambda = \int_i^f \frac{N}{\tau}\int_z^{z+\tau} 2\pi r_s B_r(z)dzdz \quad (15)$$

where N is the number of conductors per pole, and i and f are the initial and final position of the considered phase respectively. Since the back emf is given by the product of velocity v and the rate of change in flux linkage with respect to position, it is given by [6]

$$e_b = \frac{d\lambda}{dt} = \frac{dz}{dt}\frac{d\lambda}{dz} = v\frac{d\lambda}{dz} \quad (16)$$

The axial thrust is exerted on the stator winding, resulting from the interaction between the current density and the permanent magnet field. In the general position z, the thrust in an infinitesimal tubular motor length dz is given by

$$dF_z(z) = -2\pi r_s J_\theta(z) B_r^I(r_s,z)dz \quad (17)$$

It has the advantage that (17) is free from integrals of Bessel functions related to a formula $F = \int_v (\vec{J}\times\vec{B})dv$ that cause a significant analytical burden.

5.1 Single-Phase Windings

The distribution of the single-phase winding conductors cover the entire pole pitch, then i=-τ and f=0 with N=N_p. The flux linkage due to PM is

$$\lambda^{PM1} = \sum_{n=1,odd}^{\infty} \frac{8N_p r_s p[A_n^I I_1(k_n r_s) + B_n^I K_1(k_n r_s)]}{n}\sin(k_n z) \quad (18)$$

and the flux linkage due to single phase stator windings is

$$\lambda^{J1} = \sum_{n=1,odd}^{\infty}\left(\frac{32\upsilon_n\mu_0 N_p^2 r_s i_s p}{n^2\pi\tau}\bullet [-I_1(k_n r_s) + \chi_n K_1(k_n r_s)]\sin(k_n z)\right) \quad (19)$$

where p and i_s are the pole-pairs and single phase current, respectively. By substituting (18) for (16), the back emf for the tubular motor with single phase windings is obtained as:

$$e_{b1} = \sum_{n=1,odd}^{\infty} \frac{8N_p\pi r_s v p[A_n^I I_1(k_n r_s) + B_n^I K_1(k_n r_s)]}{\tau}\sin(k_n z) \quad (20)$$

From (17), the thrust for the tubular motor with single phase windings is obtained as:

$$F_{z1}(z) = -\sum_{n=1,odd}^{\infty} \frac{8\pi r_s p i_s N_p[A_n^I I_1(k_n r_s) + B_n^I(k_n r_s)]}{\tau}\cos(k_n z) \quad (21)$$

5.2 Three-Phase Windings

The distribution of each phase of the three-phase winding cover a third of the pole pitch. Eq. (15) can be applied, substituting N with $3N_t$. Then, with reference to the phase a, i=-2τ/3 and f=-τ/3. The flux linkage due to PMs is

$$\lambda^{PM3} = \sum_{n=1,odd}^{\infty}\left\{\left(24N_t\pi r_s p\cos(\frac{n\pi}{3})/n\right)\bullet[A_n^I I_1(k_n r_s) + B_n^I K_1(k_n r_s)]\right\}\sin(k_n z) \quad (22)$$

and the flux linkage due to phase **A** is

$$\lambda^{J3} = \sum_{n=1,odd}^{\infty}\left\{i_a\frac{288\upsilon_n\mu_0 N_t^2 r_s p}{\pi\tau n^2}[-I_1(k_n r_s) - \chi_n K_1(k_n r_s)]\bullet \cos\left(\frac{n\pi}{3}\right)\sin\left(\frac{n\pi}{12}\right)\sin\left(\frac{n\pi}{6}\right)\sin(k_n z)\right\} \quad (23)$$

where i_a represents the current of phase **A**. By substituting (22) for (16), the back emf per phase of the tubular motor with three phase windings is obtained as:

$$e_{b3} = \sum_{n=1,odd}^{\infty} \left\{ \left(24N_t v\pi r_s p \cos(\frac{n\pi}{3})/\tau \right) \bullet \right\} \sin(k_n z) \quad (24)$$

From (17), the thrust for the tubular motor with three phase windings is obtained as:

$$F_{z3}(z) = \sum_{n=1,odd}^{\infty} \left\{ \begin{array}{l} \left[-24\pi r_s N_t p[A_n^I I_1(k_n r_s) + B_n^I K_1(k_n r_s)]/\tau \right] \bullet \\ \left[\cos(k_n z) i_a + \cos k_n (z - \frac{2\tau}{3}) i_b + \cos k_n (z - \frac{4\tau}{3}) i_c \right] \end{array} \right\} \quad (25)$$

6. Control Parameter Estimation

6.1 Back-Emf Constant

Since the back-emf can be calculated by $e = v(d\lambda_{PM}/dz) = vK_E$, the back emf constant for the tubular motor with single phase windings is obtained from (20)

$$K_{E1} = \sum_{n=1,odd}^{\infty} 8N_p \pi r_s p[A_n^I I_1(k_n r_s) + B_n^I K_1(k_n r_s)]/\tau \quad (26)$$

In a similar manner, the back emf constant for the tubular motor with three phase windings is obtained from (24)

$$K_{E3} = \sum_{n=1,odd}^{\infty} \left\{ \left(24N_t \pi r_s p \cos(\frac{n\pi}{3})/\tau \right) \bullet \right\} \quad (27)$$

6.2 Thrust Constant

Since the thrust for the tubular motor with single phase windings can be calculated by $F_z = K_T i_s$, the thrust constant is obtained from (21)

$$K_{T1} = \sum_{n=1,odd}^{\infty} 8N_p \pi r_s p[A_n^I I_1(k_n r_s) + B_n^I K_1(k_n r_s)]/\tau \quad (28)$$

It can be observed from (26) and (28) that the back-emf constant K_{EI} is identical with thrust constant K_{TI}. However, since the thrust constant for the tubular motor with three phase windings can be calculated by $K_{T3} = 3K_{E3}/2$, it is obtained from (27)

$$K_{T3} = \sum_{n=1,odd}^{\infty} \left\{ \left(36N_t \pi r_s p \cos(\frac{n\pi}{3})/\tau \right) \bullet \right\} \quad (29)$$

6.3 Inductance

Since the inductance for the tubular motor with single phase windings is calculated by $L = \lambda_f / i_s$, it is obtained from (19)

$$L_1 = \sum_{n=1,odd}^{\infty} \frac{32\upsilon_n \mu_0 r_s N_p^2 p}{\pi\tau n^2} [-I_1(k_n r_s) + \chi_n K_1(k_n r_s)] \quad (30)$$

Since the inductance for phase A of the tubular motor with three phase windings is obtained from (23)

$$L_a = \sum_{n=1,odd}^{\infty} \left\{ \begin{array}{l} \frac{288\upsilon_n \mu_0 N_t^2 r_s p}{\pi\tau n^2} [-I_1(k_n r_s) - \chi_n K_1(k_n r_s)] \bullet \\ \cos\left(\frac{n\pi}{3}\right) \sin\left(\frac{n\pi}{12}\right) \sin\left(\frac{n\pi}{6}\right) \sin(k_n z) \end{array} \right\} \quad (31)$$

On the other hand, flux linkage due to phase A is given by

$$\begin{aligned} \lambda_a &= L_a i_a + M i_b + M i_c = L_a i_a + M(i_b + i_c) \\ &= (L_a - M) i_a = \frac{3}{2} L_a i_a \end{aligned} \quad (32)$$

Therefore, synchronous inductance is obtained as

$$L_{synch} = \frac{3}{2} L_a \quad (33)$$

7. Results And Discussion

The design parameters of the tubular linear motor are presented in Table I. Fig. 5 (a) and (b) show the comparison between analytical and FE results for the radial flux density of the tubular motor with Halbach and radial array, respectively. Fig. 6 illustrates the radial flux density due to the single and three phase currents. Both results are shown in good agreement with those obtained from FEA. Figs. 7 and 8 indicate the flux linkage and back emf for the tubular linear motor with two different arrays and winding patterns respectively. In particular, for the case when mover velocity v=100(*mm/s*), the analytical results for the back emf are compared with FE results. Fig. 9 provides a comparison of between analytical and FE results for axial thrust according to mover position of the tubular linear actuator with two different array and winding patterns. It can be seen that the thrust of the tubular linear motor with cylindrical Halbach array is superior to that with radial array.

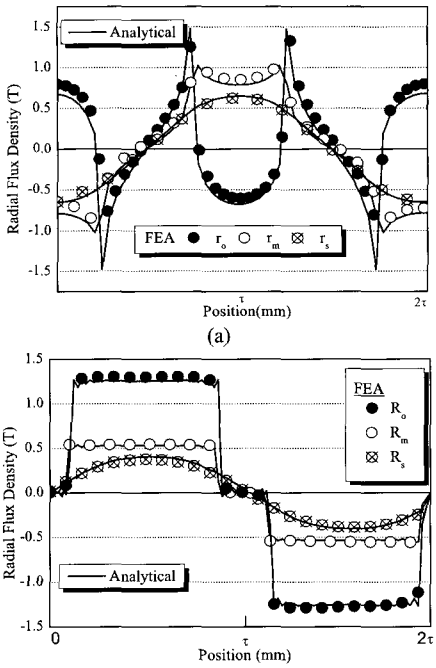

Fig. 5 Radial flux density distributions due to (a) Halbach and (b) radial magnet array.

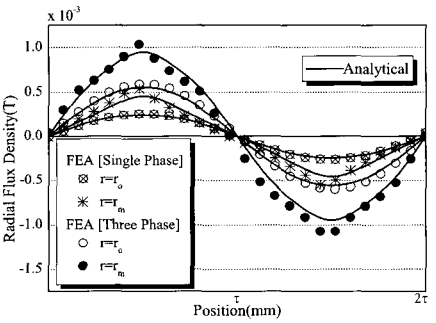

Fig. 6 Radial flux density distributions due to single- and three-phase windings.

Table 1 Design Parameters Of The Tubular Linear Motor

Parameters	Radial Magnet Array	Halbach Magnet Array
τ (pole pitch)	20(mm)	
τ_m (PM pole pitch)	15(mm)	10(mm)
r_o (inner PM radius)	10(mm)	
r_i (outer PM radius)	20(mm)	
r_s (outer air-gap radius)	25(mm)	
B_r (remanence)	1.1(T)	
p (pole number)	4 poles	4 and 1/2 poles

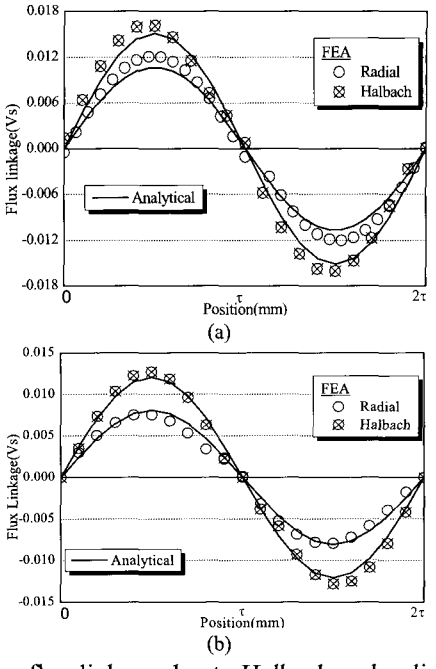

Fig. 7 The flux linkage due to Halbach and radial magnet array; (a) single-phase and (b) three-phase windings.

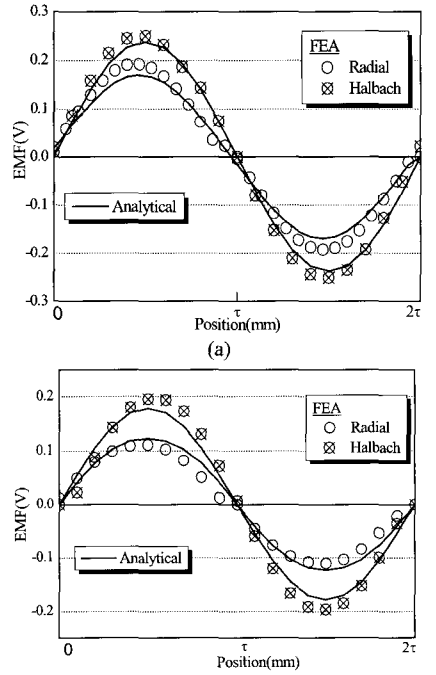

Fig. 8 The back emf due to Halbach and radial magnetized PMs; (a) single-phase and (b) three-phase windings

Table II reports the control parameters estimated by analytical solutions. Although these are not verified by FE analysis and experiments, the results presented in Table II can be regarded as reasonable because analytical solutions such as thrust, back-emf and flux linkage have already been verified extensively with FE analysis.

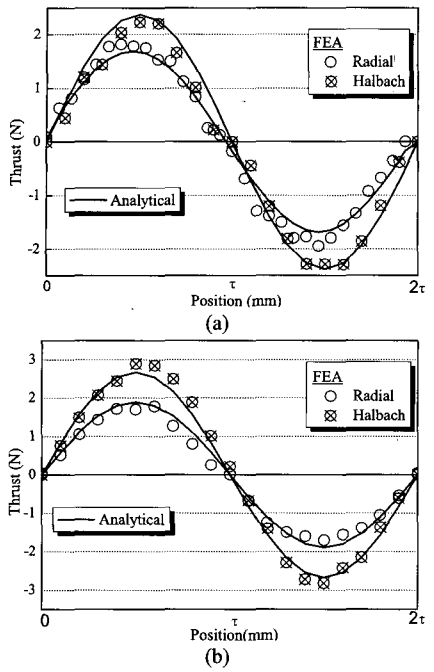

Fig. 9 Thrust on the mover with Halbach and radial magnetized PMs: (a) single-phase windings with i=1(A) and (b) three-phase windings with i_a=1(A), i_b=-0.5(A), i_c=-0.5(A).

Table 2 Estimated Control Parameters

Parameters	Radial Magnet Array		Halbach Magnet Array	
	1phase	3phase	1phase	3phase
K_T (thrust constant)	25	29.1	16.8	18.5
K_E (back emf constant)		18.4		12.3
L(inductance/pole.phase)	0.94 [mH]	0.9 [mH]	0.94 [mH]	0.9 [mH]

9. Conclusions

In this paper, analytical solutions for the magnetic fields, forces, flux linkages and back emf of tubular motor model with Halbach and radial magnetized PMs are given. The analytical results have been verified by finite element analysis, confirming the advantageousness of the proposed analysis. And then, on the basis of two-dimensional analytical solutions, control parameters required in order to perform dynamic analysis of the tubular linear motor are derived. The analytical model presented in this paper can be applicable to both slot and slotless topologies and is also very attractive in terms of rapid analysis. In our future work, on the basis of our analytical results, dynamic analysis of a tubular linear motor will be performed.

Acknowledgements

This work was financially supported by MOCIE through IERC program, Korea.

Appendix

$$\Pi_{01} = I_1(k_n r_m)K_0(k_n r_m) + I_0(k_n r_m)K_1(k_n r_m)$$

$$\Phi = \frac{\mu_0 M_{rn}}{k_n}\left(\frac{2c_2}{k_n}\Gamma - \Theta\right)$$

$$\Gamma = \omega_n{}^I I_1(k_n r_m) - K_1(k_n r_m)$$

$$\Psi = \left[\frac{2c_2\mu_0 M_{rn}}{k_n{}^2} + \frac{\mu_0 M_{zn}}{k_n}\right]\frac{1}{I_0(k_n r_o)}$$

$$\Lambda = \frac{K_0(k_n r_o)}{I_0(k_n r_o)}$$

$$\Theta = \omega_n{}^I I_0(k_n r_m) + K_0(k_n r_m)$$

$$\omega_n{}^I = -\frac{K_0(k_n r_s)}{I_0(k_n r_s)}$$

$$\Delta = \frac{2c_2\mu_0 M_{rn}}{k_n{}^2 I_0(k_n r_o)}$$

The constant coefficients of magnetic field solution for tubular linear motor with Halbach magnet array (9) are given by

$$B_n{}^I = \frac{\Psi\Pi_{01}\Theta + \left(\Phi + \frac{\mu_0 M_{zn}}{k_n}\Gamma\right)\left[K_0(k_n r_m) - \Lambda I_0(k_n r_m)\right]}{\Theta\Pi_{01}\left(\Lambda + \omega_n{}^I\right)} - \frac{2c_2\mu_0 M_{rn}}{\Theta k_n{}^2} - \frac{\mu_0 M_{zn}}{\Theta k_n}$$

$$A_n{}^I = -\omega_n{}^I B_n{}^I$$

$$A_n{}^{II} = -\frac{-\omega_n{}^I\Psi\Pi_{01} + \Lambda\left(\Phi + \frac{\mu_0 M_{zn}}{k_n}\right)}{\Pi_{01}\left[\Lambda + \omega_n{}^I\right]}$$

$$B_n{}^{II} = \frac{\Psi\Pi_{01} + \Phi + \frac{\mu_0 M_{zn}}{k_n}\Gamma}{\Pi_{01}\left(\Lambda + \omega_n{}^I\right)}$$

The constant coefficients of magnetic field solution for tubular linear motor with radial magnet array (9) are given by

$$A_n^{\ I} = -\omega_n^{\ I} B_n^{\ I}$$

$$B_n^{\ I} = \frac{\Delta\Pi_{01}\Theta + \Phi\left[K_0(k_n r_m) - \Lambda I_0(k_n r_m)\right]}{\Theta\Pi_{01}\left(\Lambda + \omega_n^{\ I}\right)} - \frac{2c_2\mu_0 M_{rn}}{\Theta k_n^{\ 2}}$$

$$B_n^{\ II} = \frac{\Delta\Pi_{01} + \Phi}{\Pi_{01}\left(\Lambda + \omega_n^{\ I}\right)}$$

$$A_n^{\ II} = \frac{-\omega_n^{\ I}\Delta\Pi_{01} + \Lambda\Phi}{\Pi_{01}\left[\Lambda + \omega_n^{\ I}\right]}$$

References

[1] W. J. Kim, M. T. Berhan, D.L. Trumper and J.H. Lang, "Analysis and Implementation of a Tubular Motor with Halbach magnet array", *IEEE,Trans. Magn.*,vol. 1, pp. 471-478, Oct. 1996.

[2] Nicola Bianchi, "Analytical Field Computation of a Tubular Permanent-Magnet Linear Motor", *IEEE Trans., Magn.*, vol. 36, pp. 3798-2801, 2000.

[3] J. Wang, G. W. Jewell, and D. Howe, "A general framework for the analysis and design of tubular linear permanent magnet machines", *IEEE Trans., Magn.*, vol. 35, pp. 1986-2000, 1999.

[4] Murray R. Spiegel, John Liu, "Mathematical Handbook of Formulas and Tables", Schaum's Outline Series, 2nd Edition, pp.152-153, 1999.

[5] David L. Trumper, Won-jong Kim, and Mark E. Williams, "Design and Analysis Framework for Linear Permanent-Magnet Machines", *IEEE,Trans. IAS*, vol. 32, pp. 371-379, 1996.

[6] Duane C. Hanselman, "Brushless Permanent-Magnet Motor Design", McGraw-Hill, pp. 70-71, 1994.

Seok-Myeong Jang

He received his B.E, M.S., and Ph.D. degrees from Hanyang University in 1976, 1978, and 1986, respectively. He is currently a Professor in the Department of Electrical Engineering, Chungnam National University. He worked as a Visiting Researcher in the Department of Electrical Engineering, Kentucky University in 1989. He is a member of KIEE. His field of interest includes design and application of linear machines, high speed machines, and linear oscillating actuators.
Tel: +82-42-821-5658

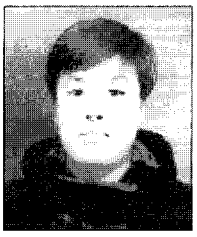

Jang-Young Choi

He was born in Korea in 1976. He received his B.S. and M.S. degrees in Electrical Engineering from Chungnam National University in 2003 and 2005. He is currently working toward his Ph.D. in the Dept. of Electrical Engineering at Chungnam National University. His research interests are design and analysis of linear machines.
Tel: +82-42-822-4933

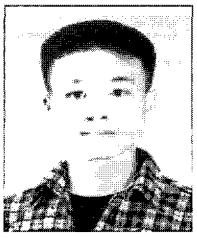

Han-Wook Cho

He was born in Korea in 1976. He received his B.S. and M.S. degrees in Electrical Engineering from Chungnam National University in 2002 and 2004. He is currently working toward his Ph.D. degree in the Dept. of Electrical Engineering at Chungnam National University. His research interests are design and analysis of high speed machines.
Tel: +82-42-822-4933

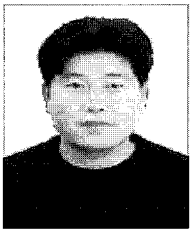

Sung-Ho Lee

He was born in Korea in 1971. He received his B.S., M.S. and Ph.D. degrees in Electrical Engineering from Chungnam National University in 1997, 1999 and 2003, respectively. His research interests are design and analysis of linear machines and automatic electric machine performance monitoring. He has worked in the LG D/A Research Lab.
Tel: +82-42-822- 4933